nature medicine

LINGO-1 antagonist promotes spinal cord remyelination and axonal integrity in MOG-induced experimental autoimmune encephalomyelitis

Sha Mi[1,7], Bing Hu[2,7,8], Kyungmin Hahm[1], Yi Luo[1], Edward Sai Kam Hui[6], Qiuju Yuan[2], Wai Man Wong[2], Li Wang[2], Huanxing Su[2], Tak-Ho Chu[2], Jiasong Guo[2], Wenming Zhang[2], Kwok-Fai So[2–4], Blake Pepinsky[1], Zhaohui Shao[1], Christilyn Graff[1], Ellen Garber[1], Vincent Jung[1], Ed Xuekui Wu[6] & Wutian Wu[2,3,5,7]

Demyelinating diseases, such as multiple sclerosis, are characterized by the loss of the myelin sheath around neurons, owing to inflammation and gliosis in the central nervous system (CNS). Current treatments therefore target anti-inflammatory mechanisms to impede or slow disease progression. The identification of a means to enhance axon myelination would present new therapeutic approaches to inhibit and possibly reverse disease progression. Previously, LRR and Ig domain–containing, Nogo receptor–interacting protein (LINGO-1) has been identified as an *in vitro* and *in vivo* negative regulator of oligodendrocyte differentiation and myelination. Here we show that loss of LINGO-1 function by *Lingo1* gene knockout or by treatment with an antibody antagonist of LINGO-1 function leads to functional recovery from experimental autoimmune encephalomyelitis. This is reflected biologically by improved axonal integrity, as confirmed by magnetic resonance diffusion tensor imaging, and by newly formed myelin sheaths, as determined by electron microscopy. Antagonism of LINGO-1 or its pathway is therefore a promising approach for the treatment of demyelinating diseases of the CNS.

In multiple sclerosis, the myelin and oligodendrocytes of brain and spinal cord white matter are the targets of T cell–mediated immune attacks[1], resulting in demyelination and the consequent progressive disabilities and paralysis. Immunomodulatory and immunosuppressive agents can slow, but not reverse, disease progression[2–4], pointing to the need to develop new treatment paradigms that involve myelin repair.

Recently, we demonstrated that LINGO-1 is a key negative regulator of oligodendrocyte differentiation and myelination[5,6]. *In vitro*, the overexpression of LINGO-1 inhibits oligodendrocyte differentiation and myelination, whereas attenuation of its function with a dominant-negative allele of *Lingo1*, *Lingo1* RNA-mediated interference, soluble LINGO-1, or LINGO-1 antagonist antibody (anti-LINGO-1) enhances oligodendrocyte differentiation and myelination[6]. LINGO-1 has been shown to have a role in oligodendrocyte differentiation and myelination *in vivo* through the analysis of *Lingo1*-knockout and transgenic mice[6,7]. These studies suggest that inhibition of LINGO-1 function could comprise a therapeutic approach for the treatment of demyelinating disease.

Myelin oligodendrocyte glycoprotein (MOG)-induced murine experimental autoimmune encephalomyelitis (EAE) is a widely accepted model for studying the clinical and pathological features of multiple sclerosis. The model has previously been used to demonstrate that fostering remyelination can be effective in moderating disease progression[4]. Approaches that enhance myelination include the promotion of oligodendrocyte precursor cell (OPC) differentiation[8–11] and the transplantation of OPCs, Schwann cells, olfactory ensheathing cells and neural stem cells into primary demyelinated lesions[12]. Here, we demonstrate that blocking LINGO-1 function, either through *Lingo1* knockout or through treatment with anti-LINGO-1, promotes functional recovery in the EAE model. Additionally, this functional recovery is correlated with improved axonal integrity and axonal myelination, as visualized by magnetic resonance diffusion tensor imaging (DTI) and electron microscopy, respectively.

Lingo1-knockout mice show earlier onset of myelination of CNS axons than the wild type, with no apparent developmental or behavioral abnormalities[6], suggesting that a LINGO-1 antagonist could be developed into an effective and specific therapeutic approach for treating demyelinating diseases. To test this hypothesis, we first determined whether *Lingo1*-knockout mice show greater resistance to the development of MOG-induced EAE than wild-type mice. An EAE score, which quantifies disease progression by measuring motor dysfunction, was used as a surrogate indicator of demyelination.

[1]Biogen Idec Inc., 14 Cambridge Center, Cambridge, Massachusetts 02142, USA. [2]Department of Anatomy, [3]State Key Laboratory of Brain and Cognitive Sciences, [4]Research Centre of Heart, Brain, Hormone and Healthy Aging, [5]Research Center of Reproduction, Development and Growth, Li Ka Shing Faculty of Medicine, and [6]Department of Electrical and Electronic Engineering, Faculty of Engineering, The University of Hong Kong, Pokfulam, Hong Kong SAR, China. [7]These authors contributed equally to this manuscript. [8]Present address: School of Life Science, The University of Science and Technology of China, Hefei, Anhui 230027, China. Correspondence should be addressed to W.W. (wtwu@hkucc.hku.hk) or S.M. (sha.mi@biogenidec.com).

Received 6 April; accepted 31 August; published online 30 September 2007; doi:10.1038/nm1664

Both wild-type (WT) and *Lingo1*-knockout mice developed EAE symptoms; however, EAE scores were significantly lower in *Lingo1*-knockout mice throughout all stages of disease progression ($P < 0.02$; **Fig. 1a**).

EAE is a complex model for demyelination, as it involves both immune and neurological components[12]. Although the evidence to date indicates a CNS-specific role for LINGO-1, the possibility remains that loss of LINGO-1 moderates EAE by altering the generation and the infiltration into the CNS of encephalogenic T cells involved in EAE pathology. These possibilities can be excluded by testing for functional differences between T cells from WT and knockout mice, followed by examination of the ability of encephalogenic T cells from WT and knockout mice to confer EAE through adoptive transfer. We isolated T cells from both WT and *Lingo1*-knockout mice after MOG immunization and measured their proliferation and cytokine release after MOG stimulation. As expected, LINGO-1 deficiency did not alter *Lingo1*-knockout T-cell responses to MOG in the proliferation assay as compared to the WT control (**Fig. 1b**). Also, there was no difference in the amounts of cytokines (interleukin (IL)-2, IL-4, IL-5, IL-6, IL-10, IL-13, IL-17, tumor necrosis factor (TNF)-α, interferon (IFN)-γ and granulocyte monocyte colony stimulating factor (GM-CSF)) released by T cells obtained from MOG stimulation of WT or *Lingo1*-knockout mice (data not shown). Consistent with normal T-cell function, MOG-immunized encephalogenic T cells isolated from *Lingo1*-knockout mice that were adoptively transferred into WT mice were able to induce EAE similarly to those from WT mice (**Fig. 1c**). In contrast, encephalogenic T cells isolated from WT mice were markedly reduced in their ability to induce EAE in *Lingo1*-knockout mice, in comparison to WT recipients ($P < 0.006$; **Fig. 1d**).

We used electron microscopy to show that lower EAE scores do indeed reflect remyelination. Characteristic 'dying-back' oligodendrogliopathy presenting as an 'inside-out' type of myelin damage[13,14] was observed more often in the demyelinated areas of WT than in those of knockout EAE mice (arrows in **Fig. 1e**). In WT mice, damaged myelin sheaths often had loose and separated layers or degraded sheath structures (arrows in **Fig. 1f**, left panel) or were completely absent (**Fig. 1g**, left panel). In contrast, *Lingo1*-knockout EAE animals showed an abundance of newly formed myelin sheaths that were notably thinner (arrowheads in **Fig. 1f**,**g**). Quantitative analysis of myelinated axons indicated that there were more myelinated fibers in *Lingo1*-knockout EAE mice than in the WT EAE controls ($P = 0.0002$; **Fig. 1h**). The combined data show that LINGO-1 deficiency probably results in an altered CNS compartment in which remyelination is encouraged. The deficiency did not influence the ability of encephalogenic T cells and inflammatory immune effector cells to cause EAE.

The mitigation of EAE progression in *Lingo1*-knockout mice suggests that exogenous means, such as the use of antibody antagonists to block endogenous LINGO-1 function, could slow EAE progression. Anti-LINGO-1 is an IgG1-isotype antibody that binds specifically to LINGO-1 (**Supplementary Fig. 1** online) to promote oligodendrocyte differentiation and myelination *in vitro* (S.M.,

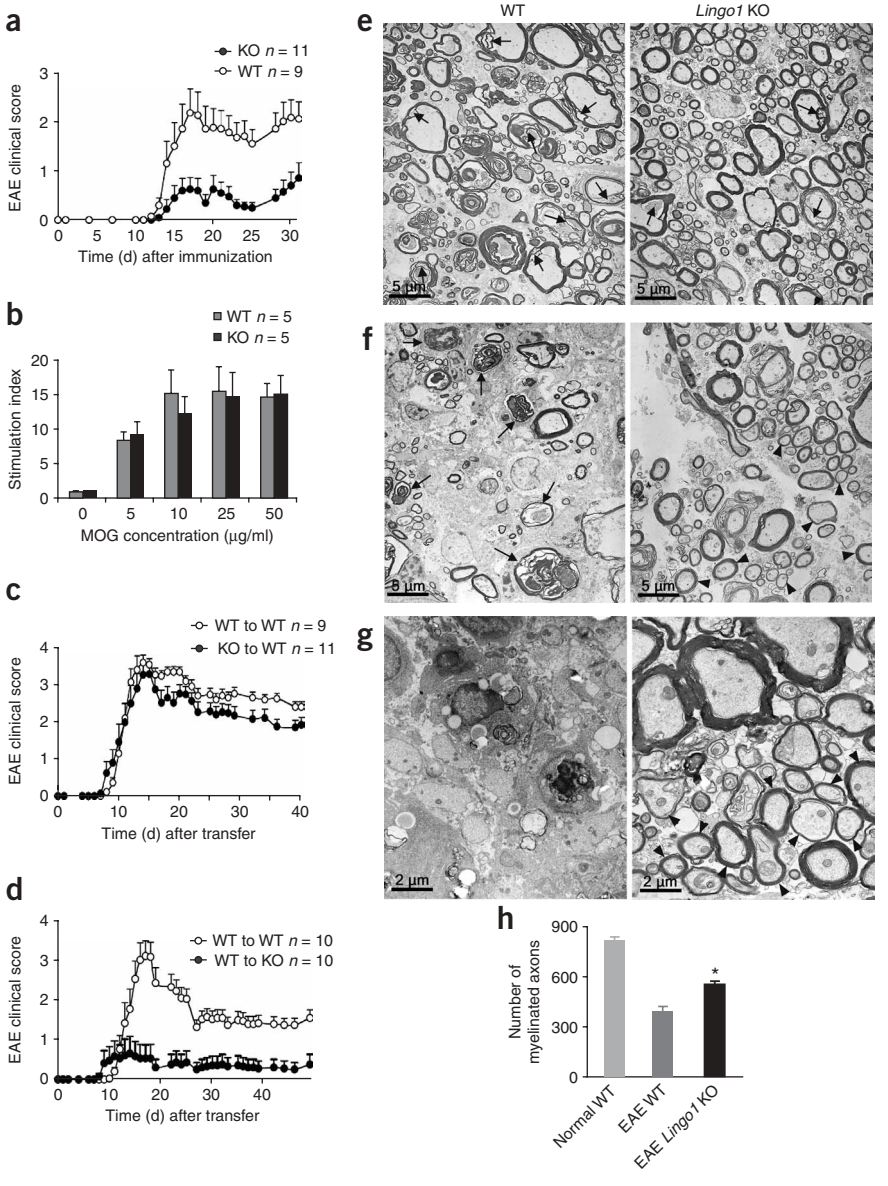

Figure 1 Lower EAE clinical scores and increased remyelination in MOG-induced EAE *Lingo1*-knockout mice. (**a**) Mean clinical scores of MOG-induced EAE in WT and LINGO-1–deficient mice. $^*P < 0.02$. (**b**) T-cell proliferation response in the presence of MOG as determined by ^{3}H-thymidine incorporation. (**c**) Adoptive transfer of EAE into WT mice by MOG-immunized encephalogenic T cells isolated from *Lingo1*-knockout or WT mice. (**d**) Adoptive transfer of EAE in *Lingo1*-knockout mice or WT mice by encephalogenic T cells isolated from WT mice. $^*P < 0.006$. (**e–g**) EM images showing remyelination in the lumbar spinal cords of *Lingo1*-knockout mice (right) and demyelination in WT control mice (left). (**h**) Quantification of toluidine blue–stained sections, showing significantly more myelinated axons in the spinal cords of *Lingo1*-knockout EAE mice ($n = 7$) than in WT EAE mice ($n = 6$). $^*P = 0.0002$. KO, knockout.

unpublished data). Here, we tested whether LINGO-1 antagonist antibody can promote functional recovery and myelination in the rat EAE model. We first determined whether the local delivery of anti-LINGO-1 can be prophylactic for the onset or the progression of EAE. Anti-LINGO-1 was introduced 3 d after MOG immunization by intrathecal delivery by osmotic pump, and the experiment was stopped after 36 d for tissue examination by histology and electron microscopy. Similarly to the results in *Lingo1*-knockout mice, anti-LINGO-1 did not alter EAE onset, but did significantly mitigate disease severity across all stages of disease progression, in comparison to an isotype antibody control or a no-treatment control, as indicated by EAE scores ($P < 0.05$; **Fig. 2a**).

Bolstered by the prophylactic data, we undertook a more clinically relevant assessment of the therapeutic potential of LINGO-1 antagonism in rats already exhibiting EAE symptoms. MOG-induced rats with EAE scores of 1.0 were treated with either anti-LINGO-1 or an isotype control antibody delivered systemically by intraperitoneal injection. After a 2-week treatment, the anti-LINGO-1 group showed significantly lower EAE scores than the control group ($P < 0.05$; **Fig. 2b**). Most notably, disease progression appeared stabilized, with a perceptible downtrend (**Fig. 2b**).

The decreased EAE severity after anti-LINGO-1 antagonist treatment indicates improved axonal function and integrity, which can be visualized by DTI. We collected DTI images of the lumbar segments of post-fixed spinal cords. Low fractional anisotropy values were obtained from the dorsal area of the spinal cord in IgG control–treated EAE rats (**Fig. 2c**, top center), which correlated with the demyelination area seen in the toluidine blue–stained section (**Fig. 2c**, bottom center). In contrast, substantially higher fractional anisotropy values were obtained from anti-LINGO-1–treated (**Fig. 2c**, top right) or normal control (**Fig. 2c**, upper left) rats, which correlated with the relatively normal myelination seen in the histological sections (**Fig. 2c**, bottom right or left, respectively). Fractional anisotropy values from projection DTI images of the anti-LINGO-1–treated group (**Fig. 2d**, right) were significantly higher than those of the IgG control–treated group (**Fig. 2d**, left, and **Fig. 2e**; $P = 0.0034$), indicating improved axonal health and remyelination. Similarly, spinal cords obtained from mice that had systemic intraperitoneal delivery of anti-LINGO-1 had higher fractional anisotropy values than the isotype antibody control group ($P = 0.0083$; **Fig. 2f**). The health of remyelinated axons was also confirmed by immunostaining for amyloid-β precursor protein (APP), a marker for axonal damage shown to be increased in multiple sclerosis lesions[15]. Fewer APP-positive elements were observed in the white matter of the anti-LINGO-1–treated EAE spinal cords than in that of the IgG control–treated cords (**Supplementary Fig. 2** online). This LINGO-1 functional antagonist therefore has potential therapeutic efficacy whether it is delivered locally or systemically and is efficacious before or after the manifestation of EAE symptoms.

We next determined whether the apparent functional improvement after anti-LINGO-1 treatment (indicated by lowered EAE scores and increased DTI image densities) correlates

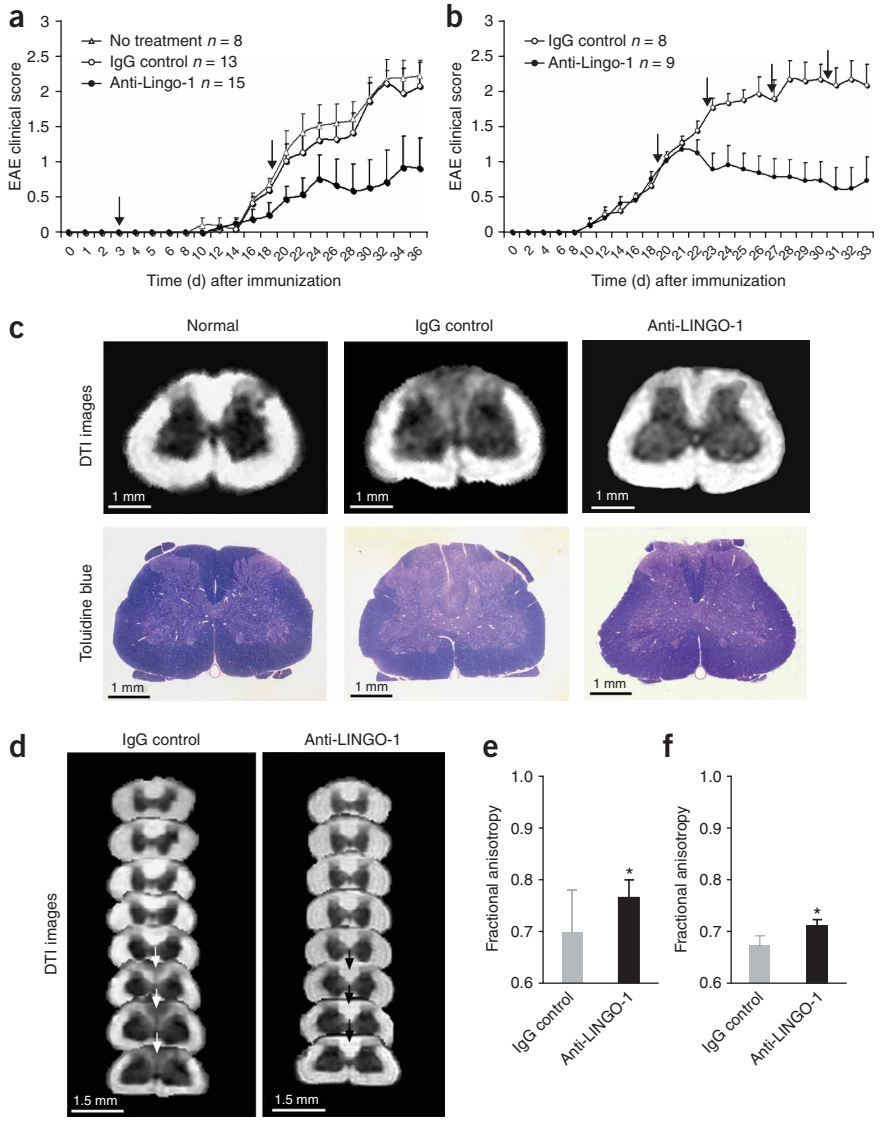

Figure 2 Treatment with an antibody antagonist to LINGO-1 function leads to functional recovery and increased integrity of axons in MOG-induced EAE rats. (**a**) Local delivery of anti-LINGO-1 or IgG control antibody, or no treatment, before the onset of clinical EAE symptoms. $P < 0.05$. (**b**) Two-week systemic treatment with anti-LINGO-1 or IgG control after the onset of clinical EAE. $P < 0.05$. Arrows indicate dosing regimen. (**c**) DTI images (top) from normal (left), IgG control–treated (center) and anti-LINGO-1–treated (right) rats matched with toluidine blue–stained semi-thin spinal cord transverse sections (bottom, from left to right, respectively). (**d**) Projection DTI images of lower thoracic and lumbar spinal cords, showing a weak DTI signal in the dorsal column of the lumbar region from IgG control–treated rats (arrows, left) and an increased DTI signal in anti-LINGO-1–treated rats (arrows, right). (**e**) Fractional anisotropy values from the dorsal spinal cord areas of rats treated by local delivery of antibody before the clinical onset of EAE symptoms ($n = 7$ in each group). $^*P = 0.0034$. (**f**) Fractional anisotropy values from the dorsal spinal cord areas of spinal cords from rats treated by systemic delivery of antibody after the clinical onset of EAE symptoms ($n = 7$ in each group). $^*P = 0.0083$.

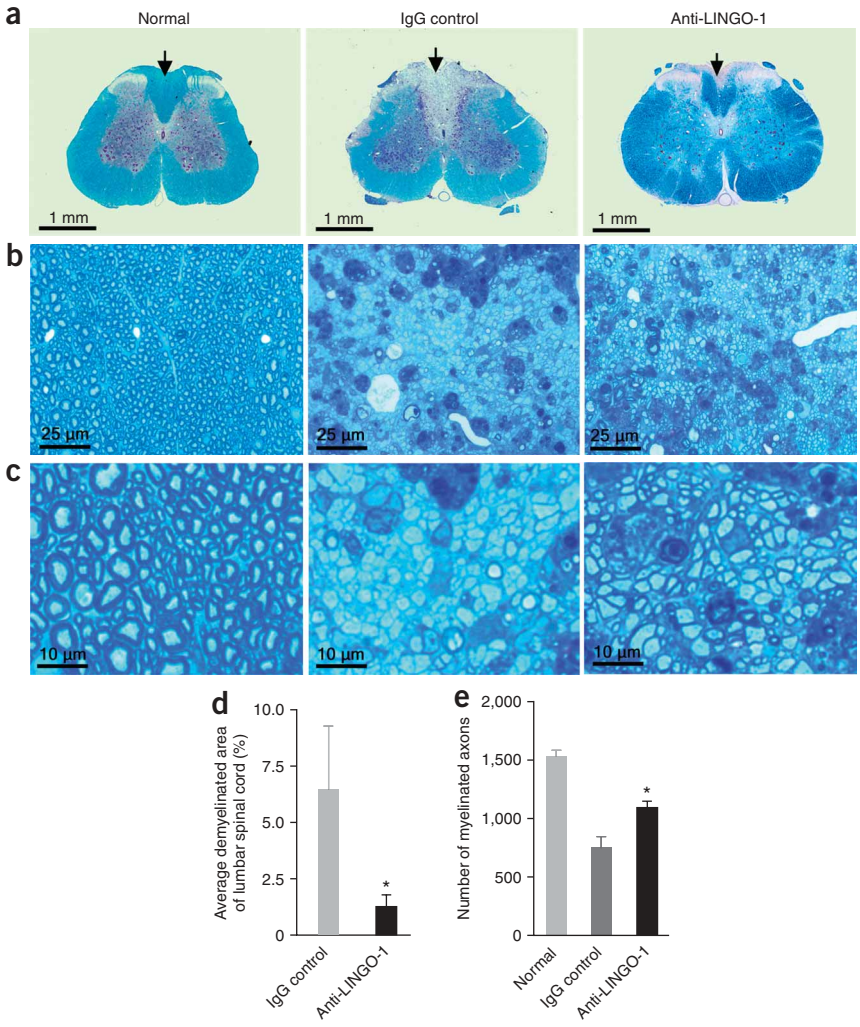

Figure 3 Histochemical detection of remyelination after LINGO-1 antibody treatment. (**a**) Paraffin spinal cord sections from normal (left), IgG control–treated (center) and anti-LINGO-1–treated (right) animals were stained with LFB. Blue areas indicate myelination, whereas pale areas indicate demyelination (arrows indicate the dorsal column of spinal cord). (**b**,**c**) Toluidine blue staining of 1-μm semi-thin sections to visualize myelination in normal (left), IgG control–treated EAE (center) or anti-LINGO-1–treated EAE (right) animals. (**d**,**e**) Anti-LINGO-1 treatment significantly reduced the demyelinated areas ($*P < 0.05$) and increased the amount of myelinated axons ($*P < 0.002$) compared to the results of IgG control treatment.

with real morphological changes in the myelination of the affected lumbar spinal cord. Luxol fast blue (LFB) staining was used to visualize myelinated regions (**Fig. 3**). In transverse paraffin spinal cord sections from normal rats (**Fig. 3a**, left), blue areas indicate intact myelin, whereas pale areas indicate demyelination. Poor LFB staining, or extensive myelin loss, was clearly evident in the control-treated animals (**Fig. 3a**, center). In contrast, increased LFB staining was seen with anti-LINGO-1 treatment (**Fig. 3a**, right). Demyelination in the lumbar spinal cord of the anti-LINGO-1–treated EAE rat group was five times lower than in the control group ($P < 0.05$, **Fig. 3d**).

Toluidine blue–stained sections were used to visualize myelinated rat axons by light microscopy (**Fig. 3b**,**c**). Loss of myelin was apparent in the control-treated axons (**Fig. 3b**,**c**, center), whereas more myelinated and/or remyelinated axons were found in anti-LINGO-1–treated rats (**Fig. 3c**, right). These newly formed myelin sheaths were thinner than those in the normal control (**Fig. 3c**, left). Quantitative analysis of myelinated axons revealed significantly fewer myelinated axons in the isotype antibody control–treated group than in the anti-LINGO-1–treated group ($P < 0.002$, **Fig. 3e**).

Electron microscopy was used to demonstrate increased axon remyelination in anti-LINGO-1–treated rats as compared to control-treated rats. After IgG control treatment, oligodendrocytes were clearly in physical contact with naked axons but were unable to re-form myelin sheaths in demyelinated white matter regions (**Fig. 4a**,**b**, left). In contrast, after anti-LINGO-1 treatment, oligodendrocytes were in contact with surrounding axons and were able to form myelin sheaths (**Fig. 4a**,**b**, right). Notably, we observed substantially more oligodentrocyte remyelination in the area closer to the site of antibody delivery than in more distant regions, which further suggests that this remyelination is specifically induced by anti-LINGO-1 (data not shown). The presence of thinly myelinated axons in demyelinated areas provides strong evidence that anti-LINGO-1 treatment promotes axon remyelination. Indeed, different remyelination phases were observed in which axons were undergoing initial wrapping, partial remyelination and almost complete remyelination (**Fig. 4c**, top) in anti-LINGO-1–treated animals. We observed a morphological structure that is typical of newly formed myelination, in which the outer (Co) and inner (Ci) ends of the spiraling cytoplasmic processes of oligodendrocytes (**Fig. 4c**, bottom left) are wrapped around axons (**Fig. 4c**, bottom left and right) in anti-LINGO-1–treated animals. Similarly, intraperitoneal delivery of anti-LINGO-1 also resulted in a considerable increase in the amount thinly remyelinated axons (data not shown).

The clinical manifestations of MOG-induced EAE, which mirror multiple sclerosis, result from an autoimmune inflammatory component and a neurological component that involves demyelination and axon loss[16]. New approaches that focus on the neurological components of myelination and axon survival are beginning to be explored[12,17,18]. In the present study, we demonstrate that diminished LINGO-1 function in mice and rats (caused by *Lingo1* knockout or treatment with LINGO-1 antagonist antibody) alleviates the symptoms of clinical neuropathology associated with MOG-induced EAE. Aside from the lower EAE scores observed in these mice and rats, physiological improvements in axonal integrity were revealed by DTI, and at the cellular level, enhanced and new myelination were revealed by histological staining and electron microscopy, respectively. The effect of LINGO-1 antagonism appears to be CNS specific, as LINGO-1 deficiency did not affect the induction phase of EAE, as shown by T-cell proliferation assays and by the release of T-cell cytokines after MOG immunization. Also, EAE can be induced by

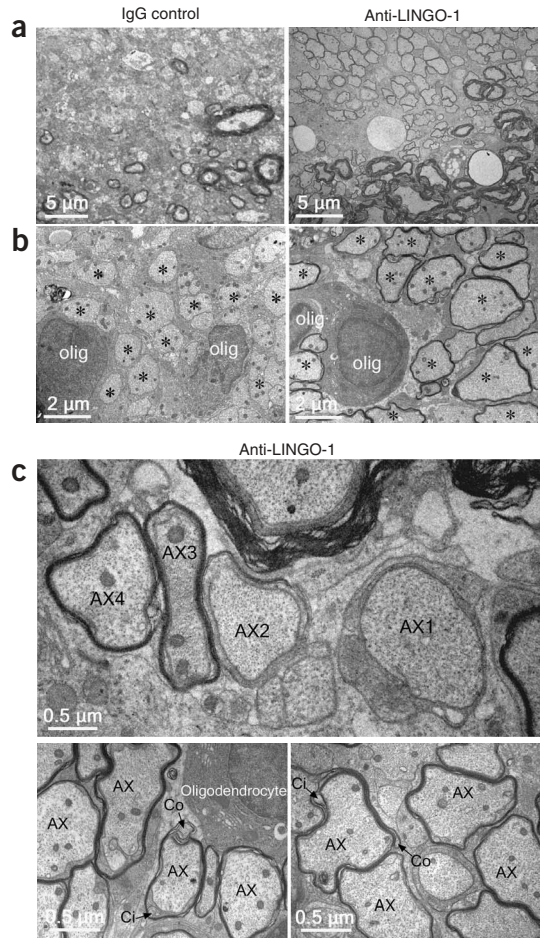

Figure 4 Electron microscopic visualization of remyelination after anti-LINGO-1 treatment. (**a**) Low-magnification electron micrographs show borders between demyelinated and myelinated areas in control-treated (left) and anti-LINGO-1–treated (right) rats. (**b**) High-magnification electron micrographs of demyelinated areas showing naked axons (asterisks) from IgG control–treated rats (left) and remyelinated axons (asterisks) in anti-LINGO-1–treated rats (right). (**c**) Top, electron micrograph of different phases of remyelination after anti-LINGO-1 treatment, with axons undergoing initial wrapping (AX1), partial remyelination (AX2) and almost complete remyelination (AX3 and AX4). Bottom, typical morphological structures of newly formed myelination are seen where the outer (Co) and inner (Ci) ends of the spiraling cytoplasmic processes of oligodendrocytes (bottom left) are wrapped around axons in anti-LINGO-1–treated animals. AX, axon.

the adoptive transfer of encephalogenic T cells from MOG-immunized *Lingo1*-knockout mice to WT mice, and EAE is mitigated when encephalogenic T cells from MOG-immunized WT mice are transferred to *Lingo1*-knockout mice. LINGO-1 inhibition's nonimmune role in the attenuation of EAE is also supported by other studies, in which it has been shown that LINGO-1 antagonist antibody promotes remyelination in two noninflammatory models of demyelination, the cuprizone and lysolecithin models (S.M., unpublished data). In demyelinated CNS, diminished LINGO-1 function is therefore likely to enhance remyelination by promoting differentiation of OPCs into mature myelin-forming oligodendrocytes. Together, these data have provided an *in vivo* proof-of-concept for the development of LINGO-1 antagonists as a novel therapeutic approach for the treatment of demyelinating diseases.

METHODS

Induction of MOG-EAE model. We induced EAE in adult rats by previously described methods[3]. Detailed procedures are provided in the **Supplementary Methods** online. All procedures were carried out according to the US National Institutes of Health Guide for the Care and Use of Laboratory Animals and were approved by the Committee on the Use of Live Animals in Teaching and Research of the University of Hong Kong and by the Biogen Idec Institutional Animal Care and Use Committee. The presence of immune cells and inflammatory infiltrates (T cells, macrophages, microglia and others) within the CNS tissue of EAE rats was detected by immunocytochemistry (**Supplementary Fig. 3** online).

Generating LINGO-1 antibody. We generated anti-LINGO-1 in mice by methods described previously[19]. Detailed procedures are provided in the **Supplementary Methods**. Cell surface–binding ELISA and competitive ELISA experiments demonstrated the specific binding to LINGO-1 (**Supplementary Fig. 1**).

Clinical evaluation of MOG-EAE and selection of animals. After MOG induction of EAE, each animal was assessed by a behavioral test based on motor functions, and an EAE score was obtained by methods described previously[3,19]. Detailed steps for the evaluation are in the **Supplementary Methods**.

T-cell function and cytokine secretion assays. We isolated cells from the draining lymph nodes of MOG-immunized mice. Five animals were used in each group. Cells were cultured in triplicate in the presence of MOG for 3 d. To measure T-cell proliferation responses, we added 1 μCi ^{3}H-thymidine to each well for the last 18 h. Cells were harvested onto filter mats using the Tomtec Harvester 96, and ^{3}H-thymidine incorporation was quantified using the Wallac 1450 Microbeta Jet counter. Duplicate cultures were set up to measure the level of cytokine secretion in the presence of 50 μg MOG. Supernatants collected 72 h after the start of the cultures were assayed for IL-2, IL-4, IL-5, IL-6, IL-10, IL-13, IL-17, TNFα, IFNγ and GM-CSF abundance using the Pierce Search Light multiplex ELISA system.

LINGO-1 antibody treatment. For local delivery, 3 d after MOG-induction, we introduced isotype control antibody or anti-LINGO-1 intrathecally into rats with a minipump (Alzet mini–osmotic pump, Alza Corporation). Each minipump held 2.6 mg anti-LINGO-1 and delivered 185 μg/d for 2 weeks, and the minipump was replaced every 2 weeks. The isotype control antibody was delivered at the same concentration and by the same method used for anti-LINGO-1.

For systemic drug delivery, we intraperitoneally injected 8 mg/kg antibody twice per week (either anti-LINGO-1 or isotype control antibody), commencing when an EAE score of 1.0 was reached. The rats were killed after 2 weeks of treatment.

Tissue preparation for DTI, electron microscopy and histology. Animals were perfused with a fixative 30 and 36 d after MOG-EAE induction for mice and rats, respectively, by the method described previously[20]. Fixed tissues were prepared for DTI (see below), immunocytochemistry and electron microscopy by methods described previously[16,20,21].

Quantification of demyelination area and axon preservation. Areas of demyelination were estimated on complete transverse LFB–stained spinal cord sections (lumbar 4 segments, L4). Blue areas indicate intact myelin, whereas pale areas indicate demyelination (**Supplementary Fig. 4a** online). ImageJ software (free software from the US National Institutes of Health) was used to manually trace the total cross-sectional area (yellow trace, **Supplementary Fig. 4b**) and the demyelination area (red trace, **Supplementary Fig. 4b**) of each section. Demyelination was expressed as a percentage of the total demyelination area over the total spinal cord area, using random sections from the fourth lumbar segment of each animal.

To quantify axons, we adopted a line-sampling method similar to that described previously[16]. Axons intercepted by nine fixed sampling lines (red lines, **Supplementary Fig. 5** online) were sampled from toluidine blue–stained

1-μm-thick sections of the L4 spinal segment of each rat. Nine tissue strips extending from the gray matter to the pial surface were selected under the ×100 oil-immersion objective of a Zeiss microscope. All myelinated axons whose axoplasms were intercepted by a sampling line were counted. Sampled axonal profiles from the tissue strips of each rat were pooled. Because of the resolution limits of light microscopy, unmyelinated and myelinated fibers of cross-sectional areas smaller than 0.1 μm^2 were not included in the counts.

Diffusion tensor magnetic resonance imaging. All magnetic resonance imaging experiments were performed on a high-field small-bore 7 Tesla rodent magnetic resonance imaging scanner (70/16 PharmaScan, Bruker Biospin GmbH) at the University of Hong Kong. DTI was used for semi-quantification of the demyelination area in the spinal cord of EAE rats as described previously[22–24]. Detailed procedures are provided in the **Supplementary Methods**.

Statistical analysis. GraphPad Prism (version 4.0, GraphPad) software was used for statistical analysis. Data are shown as means ± s.e.m. Statistical significance in comparing two means was tested with the unpaired Student's *t*-test (with Welch's correction or Mann-Whitney modification). One-way analysis of variance was applied to test multiple means. $P < 0.05$ was set as the cutoff for statistical significance.

Note: Supplementary information is available on the Nature Medicine website.

Published online at http://www.nature.com/naturemedicine
Reprints and permissions information is available online at http://npg.nature.com/reprintsandpermissions

1. Trapp, B.D., Ransohoff, R.M., Fisher, E. & Rudick, R. Neurodegeneration in multiple sclerosis: relationship to neurological disability. *Neuroscientist* **5**, 48–57 (1999).
2. Noseworthy, J.H., Gold, R. & Hartung, H.P. Treatment of multiple sclerosis: recent trials and future perspectives. *Curr. Opin. Neurol.* **12**, 279–293 (1999).
3. Diem, R. *et al.* Combined therapy with methylprednisolone and erythropoietin in a model of multiple sclerosis. *Brain* **128**, 375–385 (2005).
4. DuboisDalcq, M., ffrench-Constant, C. & Franklin, R.J.M. Enhancing central nervous system remyelination in multiple sclerosis. *Neuron* **48**, 9–12 (2005).
5. Mi, S. *et al.* LINGO-1 is a component of the Nogo-66 receptor/p75 signaling complex. *Nat. Neurosci.* **7**, 221–228 (2004).
6. Mi, S. *et al.* LINGO-1 negatively regulates myelination by oligodendrocytes. *Nat. Neurosci.* **8**, 745–751 (2005).
7. Lee, X. *et al.* NGF regulates the expression of axonal LINGO-1 to inhibit oligodendrocyte differentiation and myelination. *J. Neurosci.* **27**, 220–225 (2007).
8. Wekerle, H., Kojima, K., Lannes-Vieira, J., Lassmann, H. & Linington, C. Animal models. *Ann. Neurol.* **36** Suppl, S47–S53 (1994).
9. Kerschensteiner, M. *et al.* Remodeling of axonal connections contributes to recovery in an animal model of multiple sclerosis. *J. Exp. Med.* **200**, 1027–1038 (2004).
10. Reynolds, R. *et al.* The response of NG-2 expressing oligodendrocyte progenitors to demyelination in MOG-EAE and MS. *J. Neurocytol.* **31**, 523–536 (2002).
11. Ben-Hur, T. *et al.* Transplanted multipotential neural precursor cells migrate into the inflamed white matter in response to experimental autoimmune encephalomyelitis. *Glia* **41**, 73–80 (2003).
12. Lubetzki, C., Williams, A. & Stankoff, B. Promoting repair in multiple sclerosis: problems and prospects. *Curr. Opin. Neurol.* **18**, 237–244 (2005).
13. Ludwin, S.K. & Johnson, E. Evidence for a "dying-back" gliopathy in demyelinating disease. *Ann. Neurol.* **9**, 301–305 (1981).
14. Lassmann, H., Bartsch, U., Montag, D. & Schachner, M. Dying-back oligodendrogliopathy: a late sequel of myelin-associated glycoprotein deficiency. *Glia* **19**, 104–110 (1997).
15. Trapp, B.D. *et al.* Axonal transection in the lesions of multiple sclerosis. *N. Engl. J. Med.* **338**, 278–285 (1998).
16. Papadopoulos, D., Pham-Dinh, D. & Reynolds, R. Axon loss is responsible for chronic neurological deficit following inflammatory demyelination in the rat. *Exp. Neurol.* **197**, 373–385 (2006).
17. Kornek, B. *et al.* Multiple sclerosis and chronic autoimmune encephalomyelitis: a comparative quantitative study of axonal injury in active, inactive, and remyelinated lesions. *Am. J. Pathol.* **157**, 267–276 (2000).
18. Zhao, C., Fancy, S.P.J., Kotter, M.R., Li, W.W. & Franklin, R.J.M. Mechanisms of CNS remyelination—the key to therapeutic advances. *J. Neurol. Sci.* **233**, 87–91 (2005).
19. Eager, K.B. & Kennett, R.H. The use of conventional antisera in the production of specific monoclonal antibodies. *J. Immunol. Methods* **64**, 157–164 (1983).
20. Wu, W., Scott, D.E. & Reiter, R.J. Transplantation of mammalian pineal gland: studies of survival, revascularization, reinnervation, and recovery of function. *Exp. Neurol.* **122**, 88–99 (1993).
21. Li, L. *et al.* Rescue of adult mouse motoneurons from injury-induced cell death by a glial cell line-derived neurotrophic factor (GDNF). *Proc. Natl. Acad. Sci. USA* **92**, 9771–9775 (1995).
22. Hasan, K.M., Gupta, R.K., Santos, R.M., Wolinsky, J.S. & Narayana, P.A. Comparison of gradient encoding schemes for diffusion-tensor MRI. *J. Magn. Reson. Imaging* **13**, 769–780 (2001).
23. Basser, P.J. & Pierpaoli, C. Microstructural and physiological features of tissues elucidated by quantitative-diffusion-tensor MRI. *J. Magn. Reson. B.* **111**, 209–219 (1996).
24. Kim, J.H. *et al.* Detecting axon damage in spinal cord from a mouse model of multiple sclerosis. *Neurobiol. Dis.* **21**, 626–632 (2006).